nature immunology

Surface-bound chemokines capture and prime T cells for synapse formation

Rachel S Friedman, Jordan Jacobelli & Matthew F Krummel

T cell activation *in vivo* occurs in a lymphoid milieu that presents chemotactic and T cell receptor signals concurrently. Here we demonstrate that T cell zone chemokines such as CCL21 are bound to the surface of lymph node dendritic cells. Contact with antigen-presenting cells bearing chemokines costimulated T cells by a previously unknown two-step contact mechanism. T cells initially formed an antigen-independent 'tethered' adhesion on chemokine-bearing antigen-presenting cells. The formation of those tethers superseded T cell receptor signaling and immunological synapse formation. However, chemokine-tethered T cells were hyper-responsive to subsequent contacts with antigen-presenting cells. Thus, T cells are costimulated '*in trans*' and sequentially after initial engagement with their chemokine-rich environment.

The motility and positioning of naive T cells in lymph node is modulated by antigen-independent cues as well as antigen-specific signaling. In the absence of antigen, T cells participate in multiple modes of motion, including a 'random walk', a seemingly directed 'torpedo mode' and a tethered or slowly motile mode with activity at the leading edge[1]. Early engagements with peptide-bearing dendritic cells (DCs) are associated with increasingly confined paths with more frequent turns but little variation in overall motility rather than immediate T cell arrest[1–3]. These activities occur in the T cell zone, where chemokines such as the CCR7 ligands CCL21 (also called secondary lymphoid chemokine) and CCL19 (also called EBI1 ligand chemokine and MIP-3β) are present at high concentrations[4].

In contrast to the large range of responses to antigen-bearing antigen-presenting cells (APCs) noted *in vivo*, *in vitro* T cell activation in the absence of chemokines proceeds directly to a stable interaction. Contact of T cells with antigen-bearing APCs typically results in immediate firm adhesion, followed by calcium signaling[5], tyrosine phosphorylation[6] and associated microclustering of the T cell receptor (TCR)[7–9] within the first 2 min. Coalescence of TCR clusters in this 'immature' synapse give rise to a 'mature' immunological synapse with a characteristic central supramolecular activating cluster of TCRs surrounded by concentric rings of adhesion and auxiliary molecules[7,10]. Of particular note is that initial peptide–major histocompatibility complex (MHC) recognition results in T cell arrest. The T cell 'stop' signal derives directly from TCR signaling[11], resulting in calcium release[12], which can then initiate a range of events, including myosin II heavy chain phosphorylation[13].

A factor that probably influences the transition from motile to 'stopped' activity is chemokines in the T cell zone. Studies of lymphocytes under flow have shown that many T cell chemokines aid in arrest because of their transient upregulation of β_2 integrin binding[14–16]. CCR5 and CCR7 ligands 'costimulate' T cell activation in proliferation assays[17,18]; however, the mechanism for this costimulation is not fully understood. Costimulation by CCR7 ligands is unexpected[18], as soluble gradients of secondary lymphoid chemokines such as CCL19 and CCL21 induce transmigration past a TCR-stimulatory surface, thereby preventing T cell activation[19].

In addition to inducing transmigration when in solution, chemokines are highly charged small molecules that are readily adsorbed onto the extracellular matrix and cell surfaces[20]. Surface-presented chemokines may be a more potent form of ligand[21,22]. For example, lymphocytes are captured on surfaces bearing intercellular adhesion molecule 1 (ICAM-1) in the presence of chemokines[23], and indeed binding is more efficient when chemokines are presented together on the same surface[22]. It has been suggested that this occurs because of improved capture of short-lived affinity-upregulated integrins in the vicinity of triggered chemokine receptors[22]. Presentation of chemokine on an integrin-bearing surface in the presence of antigen-MHC recognition gives rise to increased adhesion to artificial lipid bilayers[23]. However, the physiological relevance and resulting T cell response to chemokines 'presented' in the T cell zone has not been assessed in the context of the cellular response to TCR engagement.

Here we present data that unify many of those observations. In studies of the effects of chemokines on antigen-recognition in real time, we show that specific recognition of these molecules occurred when they were bound to the surfaces of APCs. After contact of a T cell with a chemokine-bearing APC, a chemokine-mediated tether was established, resulting in a distinct phase of interaction. That first step did not support TCR signaling but instead captured the T cell in a state in which its leading edge projected and retracted until it found a suitable new surface. Establishment of that contact enhanced T cell sensitivity to antigen, as antigen-dependent conjugate formation was

The Department of Pathology, University of California at San Francisco, San Francisco, California 94143, USA. Correspondence should be addressed to M.F.K. (matthew.krummel@ucsf.edu).

Received 21 June; accepted 28 July; published online 10 September 2006; corrected after print 29 September 2006; doi:10.1038/ni1384

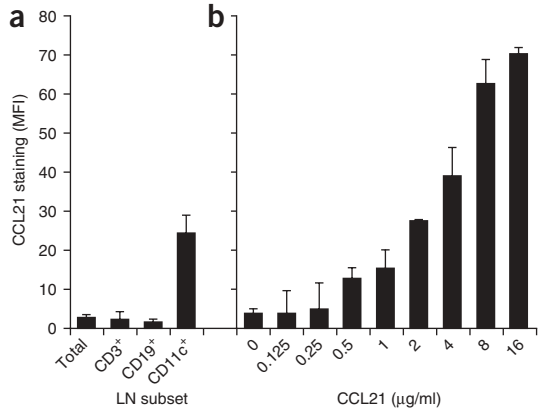

Figure 1 CCL21 is stably bound to the surface of lymph node–derived DCs. (**a**) Flow cytometry of staining for cell surface–bound CCL21 on lymph node cell subsets (horizontal axis). (**b**) Flow cytometry of staining for cell surface–bound CCL21 on the A20 B cell line pulsed with CCL21 (concentration, horizontal axis) and then washed. The mean fluorescent intensity (MFI) of control staining with secondary antibody alone is subtracted as the background for each condition (**a**,**b**). Data are representative of three experiments; error bars, s.d. of duplicate samples.

more robust during subsequent antigen stimulation, even when the chemokine and antigen were presented on separate APCs. Thus, '*trans*' costimulation by means of chemokine-initiated tethering and priming allows microenvironmental cues to modulate T cell reactivity.

RESULTS

Lymph node DCs bear stably bound CCL21

To begin to study how APC-bound chemokines modulate T cell reactivity, we measured CCL21 on lymph node DCs *ex vivo*. We stained the surfaces of freshly isolated lymph node cells with antibody to CCL21 (anti-CCL21). Although the total lymph node population showed low intensity of specific staining, $CD11c^+$ DCs showed high specific staining, indicating substantial immobilized CCL21 on their surface (**Fig. 1a**). In contrast, T cells and B cells, although they had reproducible staining, had approximately 6–12% of the staining of $CD11c^+$ DCs. Staining with a goat IgG isotype control antibody showed less than 5% of the specific staining seen with anti-CCL21 (data not shown).

To determine the effect of the surface-bound CCL21 on T cell–APC interactions, we established a model with which we could add surface-bound CCL21 to antigenic APCs. The A20 B cell line served as an APC with minimal expression of CCL21 on its surface that stably bound CCL21 in a dose-dependent way (**Fig. 1b**). Based on that titration, A20s pulsed with 2 μg/ml of CCL21 approximated the quantity on the surface of lymph node DCs.

Surface-bound CCR7 ligands induce tethering of T cells to APCs

To examine the effects of chemokines on early T cell–APC interactions, we compared the dynamics and morphology of the contacts using real-time differential interference contrast (DIC) and calcium imaging. Initially we used DO11.10 T cell blasts, as their immunological synapse phenotype in response to APCs without chemokines has been characterized extensively. We 'loaded' T cells with the calcium-sensitive dye Fura-2, AM (Fura-2AM) and mixed them with A20 B cells in the presence or absence of exogenously added chemokine. We initially explored the effects of chemokine added in solution and found that those effects were induced by triggering of CCR7 on T cells by APC-bound chemokine (**Fig. 2**).

In contrast to immunological synapse formation with antigen but without chemokines (**Supplementary Video 1** online), T cells interacting with APCs in the presence of CCL21 (**Fig. 2a** and **Supplementary Video 2** online) or CCL19 (data not shown) but in the absence of antigen contacted the APC with their leading edge, but did not initiate calcium signaling or round up. Those cells continued to crawl along the APC, but rather than crawling away, the T cells remained attached to the APC by a uropodal tether. This tether typically persisted for minutes in the absence of additional cell contacts. During such engagements, the leading edge continued to ruffle and extend pseudopodial protrusions as if the cell were trying to crawl away but was prevented from doing so by an adhesion at its uropod. To determine the frequency of chemokine-induced T cell tethering, we quantified those data (**Fig. 2b**). We defined 'tethering' as the presence of a polarized amoeboid T cell adhered to an APC by its uropod. CCL21 and CCL19 induced tethering in 68% and 45% of DO11.10 T cell blasts that contacted an APC, compared with the background of 21% tethering in the absence of exogenously added chemokine. Background tethering may be modulated by activating stimuli other than chemokines, such as the interleukin 2 used in T cell blast cultures.

The observations reported above could be explained by increased adhesiveness due to CCR7 signaling in either the T cell or the APC. To test whether tethering resulted from CCR7 signaling in the T cell, we compared wild-type and CCR7-deficient T cell blasts. We quantified tethering from real-time microscopy of T cell morphology and interactions. CCL21 induced significant tethering to APCs in wild-type T cells ($P = 2.53 \times 10^{-12}$) but not in CCR7-deficient T cells ($P = 0.7$), indicating that tethering is induced by CCR7 signaling in the T cell and not in the APC (**Fig. 2c**).

Given the presence of surface-bound CCL21 on lymph node–derived DCs (**Fig. 1**), we hypothesized that those observations were due to interactions of T cells with chemokines bound to the APC surface. To address that, we prepulsed T cells or A20 B cell APCs with CCL21 and washed away unbound chemokine. We compared the resulting antigen-independent tethering to that produced by the addition of chemokine to the culture. Surface-bound CCL21 pulsed onto the APCs was sufficient to achieve the maximum tethering obtained with chemokine added to the culture (**Fig. 2d**). In contrast, CCL21 prepulsed onto T cells did not induce associations with APCs significantly beyond the tethering obtained in the absence of added chemokines ($P = 0.42$). Along with the CCR7-knockout data (**Fig. 2c**), this result showed that the augmented adhesion was a response to surface-bound chemokines presented by APCs to T cells.

Finally, although we focused our study on the CCR7 ligands, we used a flow cytometry–based cell-coupling assay to detect adhesion of T cells to APCs in the presence of various T cell chemokines. We incubated DO11.10 T cell blasts with A20 B cell APCs in the presence or absence of 1 μg/ml of chemokine. After incubating the cells for 1 min at 37 °C, we fixed the cells and quantified the proportion of T cell–APC couples (**Fig. 2e**). The CCR7 ligands CCL21 ($P = 0.007$) and CCL19 ($P = 0.005$) induced the strongest adhesion of T cells to APCs, whereas the chemokines CXCL10 ($P = 0.02$), CCL5 ($P = 0.05$) and CXCL12 ($P = 0.03$) induced lower but significant adhesion of T cells to APCs. CCL3 ($P = 0.3$) and CCL17 ($P = 0.2$) did not mediate significant adhesion to APCs. Although these results do not control for physiological expression or for the potential for variation in receptor expression on T cells, they indicate that a range of T cell chemokines can capture T cells on APCs.

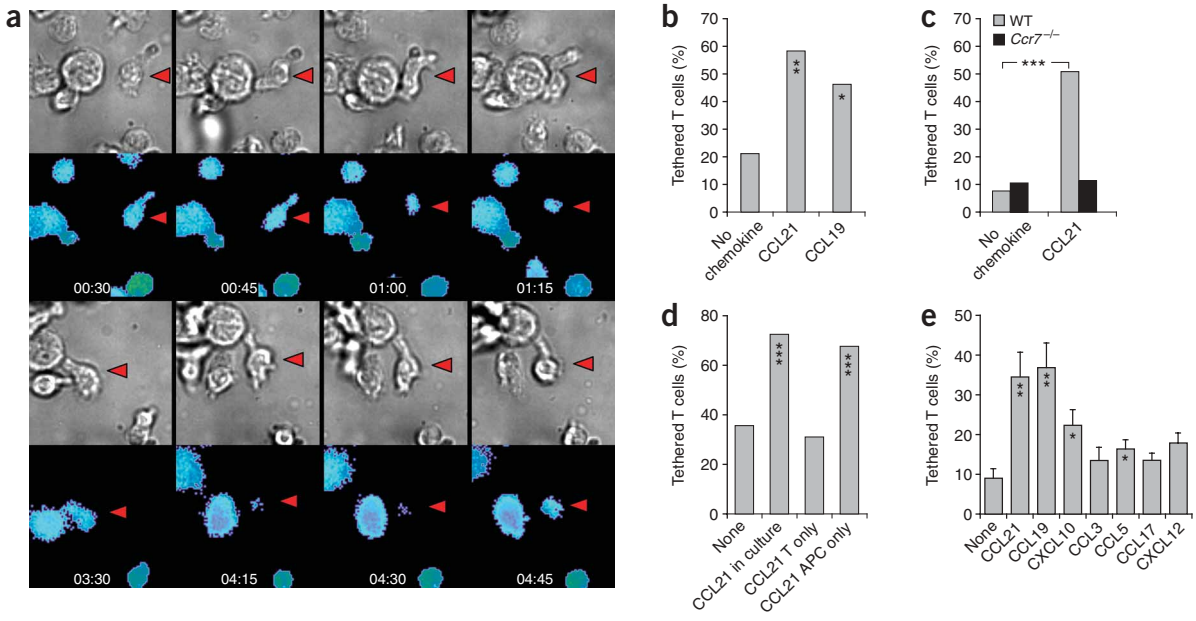

Figure 2 Surface-bound chemokines induce antigen-independent tethered adhesion of T cells to APCs. (**a**) Time-lapse series of DIC images (top and third rows) and Fura-2AM calcium images (second and bottom rows) of labeled T cell blasts interacting with A20 B cell APCs in the presence of 1 μg/ml of CCL21 (from **Supplementary Video 2**). The T cell of interest (red triangles) tethers to an APC. Calcium flux is on a 'pseudocolor' scale indicating the ratio of Fura-2AM emissions at 340 nm to those at 380 nm. Time elapsed is in min:s. Original magnification, ×40. (**b–d**) Quantification of tethering of T cells to A20 B cell APCs. *, $P < 0.05$, **, $P < 0.001$, ***, $P < 1 \times 10^{-9}$, versus no chemokine (χ^2 test). (**b**) DO11.10 T cell blasts in the presence or absence of 1 μg/ml of CCL21 or CCL19. Data were quantified by an independent party 'blinded' to sample identity. Data are representative of three experiments ($n > 30$ cells per condition). (**c**) Wild-type (WT) and *Ccr7*$^{-/-}$ C57BL/6 T cell blasts in the presence or absence of 1 μg/ml of CCL21. Data are pooled from two experiments ($n > 100$ cells per condition). (**d**) DO11.10 T cells blasts incubated with 1 μg/ml of CCL21 in culture, or with 1 μg/ml of CCL21 pulsed onto T cells or APCs, and then washed. Data are pooled from three experiments ($n > 100$ cells per condition). (**e**) Interaction of DO11.10 T cell blasts and A20 B cell APCs incubated together with no chemokine or 1 μg/ml of various chemokines (horizontal axis), assessed by flow cytometry at 1 min. Error bars, s.e.m. of three experiments done in duplicate. *, $P \leq 0.05$, and **, $P \leq 0.01$, versus no chemokine (two-tailed Student's *t*-test). Data are representative of eight (**a**), three (**b**), two (**c**) or three (**d**,**e**) experiments.

Chemokines induce a two-step dynamic of T cell activation

When T cells contacted APCs bearing both CCL21 and agonist peptide-MHC, the tether phenotype initially dominated (**Fig. 3a**,**b** and **Supplementary Video 3** online). T cells engaging such APCs initially continued to crawl and failed to round up, but remained attached by their uropods. As in the chemokine-only case, the leading edge continued to be highly active and the cells failed to flux calcium. However, when the leading edge subsequently engaged another surface bearing peptide-MHC, the uropodal tether was rapidly released, calcium infux occurred and a conventional immunological synapse resulted. The second contact could be on the same APC, *in cis*, as shown by the T cell indicated with the green triangle (**Fig. 3a**), which flipped around on itself and contacted the APC on which it was tethered with its uropod and leading edge simultaneously. After this second contact, it formed an immunological synapse on the APC. Alternatively, the second contact could be on a separate APC, *in trans*, as shown by the T cell identified by the red triangle (**Fig. 3a**). This T cell contacted a neighboring APC with its leading edge, inducing release of the tether and formation of an immunological synapse on that neighboring APC. Quantification of this transition showed that there was rarely a two-step 'tether-to-synapse' dynamic in the absence of added chemokine but that this was the main mode of association in the presence of CCL21 (**Fig. 3b**). In the presence of antigen, CCL19 also promoted a two-step activation process that was similar to that induced by CCL21, although at lower frequency (data not shown). Additionally, T cell blasts showed two-step activation in the absence of exogenously added chemokines when incubated with mature, bone marrow–derived DCs presenting cognate antigen (**Supplementary Video 4** online), which is likely to be attributable to CCL19 on their surface.

The transition from a chemokine-dependent tether to an antigen-dependent immunological synapse consistently and rapidly produced a functional calcium signal (**Fig. 3a**). To quantify that transition, we undertook kinetic analysis of antigen- and CCL21-mediated T cell–APC coupling. We used the flow cytometry–based cell-coupling assay described above to quantify T cell–APC couples over time. We used pelleted cultures for this assay, as they might better simulate the packed environment of the lymph node. DO11.10 T cell blasts incubated with APCs and CCL21 underwent transient chemokine-dependent, antigen-independent adhesion during the first minute of encounter (**Fig. 3c**). Although this assay does not detect morphology, we believe that this adhesion represents the tethered morphology we noted by microscopy. In the presence of chemokine alone, this adhesion rapidly dissipated over 5 min and was gone by 15 min after incubation. In contrast, encounter of APCs bearing only antigen resulted in a slow accumulation of couples over the 45-minute time course. The combination of CCL21 and antigen resulted in both increased initial adhesion and then a subsequent antigen-dependent maintenance of the coupling at later times, supporting the idea of the mechanism of two-step activation noted by microscopy. Over the entire time course, coupling frequency in the presence of antigen plus CCL21 remained greater than that achieved with antigen alone, suggesting that chemokines help to break down the barriers to synapse formation.

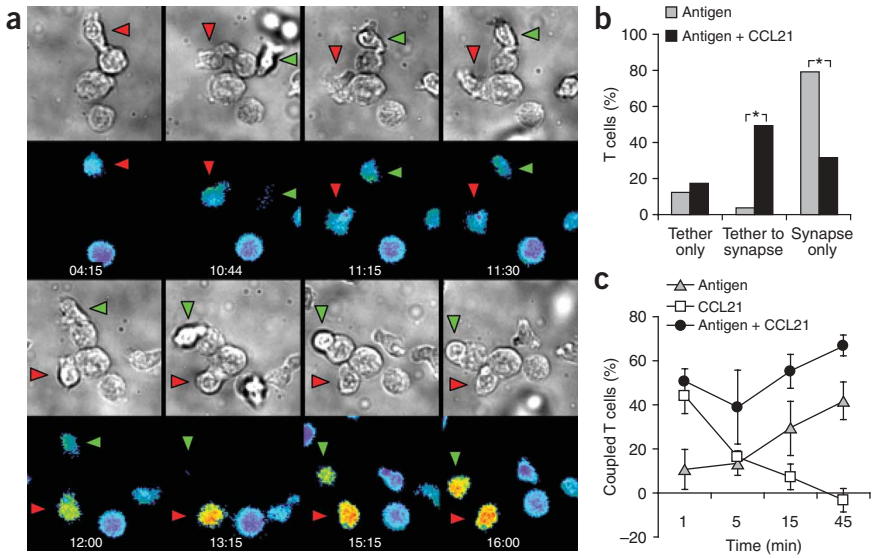

Figure 3 CCL21 mediates a two-step dynamic of T cell activation with a tethered intermediate that leads to augmentation of antigen-specific coupling. (**a**) Time-lapse series of DIC images (top and third rows) and calcium flux images (second and bottom rows) of DO11.10 T cell blasts and A20 B cell APCs incubated with 1 μg/ml of OVA peptide and 1 μg/ml CCL21 (from **Supplementary Video 3**). The T cells of interest (red and green triangles) undergo a two-step dynamic of activation. Calcium flux and time elapsed as in **Figure 2a**. Original magnification, ×40. Data are representative of three experiments. (**b**) Quantification of two-step T cell activation on A20 B cell APCs in the presence of 1 μg/ml of OVA peptide (Antigen) and the presence or absence of 1 μg/ml of CCL21. Data were quantified by an independent party 'blinded' to sample identity. *, $P \leq 0.0001$, versus samples incubated with antigen alone (χ^2 test). Data are representative of three experiments ($n \geq 30$ cells per condition). (**c**) Interaction of DO11.10 T cell blasts and A20 B cell APCs incubated together in the presence or absence of 1 μg/ml of OVA peptide and/or 1 μg/ml of CCL21 (time, horizontal axis), assessed by flow cytometry. For normalization between experiments, values for coupling in the absence of added chemokine or peptide are subtracted as background. Error bars, s.d. of three experiments.

Tethering primes T cells for antigenic stimulation '*in trans*'

Given the increases in antigen-dependent couple formation (**Fig. 3c**) and the two-step process of interactions (**Fig. 3a**), we speculated that the tether might prime T cells for more robust interactions with neighboring antigen-bearing APCs. To test whether the tether was sufficient to augment the efficiency of synapse formation (**Fig. 4**), we created an assay in which we provided the chemokine and TCR stimuli on the surface of separate APCs. We assessed antigen-specific coupling by the flow cytometry coupling assay after 15 min of incubation, at which time tethering had dissipated. CCL21 augmented antigen-dependent coupling when presented together with antigen on the same APC '*in cis*' (**Fig. 4a**). Notably, APCs bearing only immobilized CCL21 were capable of augmenting coupling in response to a separate set of APCs bearing only antigen '*in trans*' (**Fig. 4a**). This *trans* costimulation was probably due to the T cell capture events we have described, but it could have been due to chemokines' being shed and taken up by adjacent antigen-bearing cells. Indeed, to a small extent that occurred, as demonstrated by staining for surface-bound CCL21 after incubation of the two APC populations together in assay conditions (**Fig. 4b**). However, that transfer was abrogated by fixation of the APCs with 1% paraformaldehyde before incubation of the cells together (**Fig. 4d**). A coupling assay of APCs fixed with 1% paraformaldehyde confirmed that the augmentation of coupling '*in trans*' occurred in the absence of transferred CCL21 (**Fig. 4c**). More than 90% of coupled T cells were bound to antigen-bearing APCs, confirming the antigen specificity of the CCL21-mediated augmentation (data not shown). Along with the results presented in **Figure 3**, these results strongly supported the idea of chemokine-mediated tethering as a priming event for TCR signaling.

LFA-1–ICAM interactions are required for tether formation

To understand the nature of the tether phenotype, we assessed adhesion and signaling (**Fig. 5**). We tested the ability of a series of antibodies to integrins to block chemokine-induced tethers. Only blocking antibody to the integrin LFA-1 had a significant effect on tether formation ($P = 1.3 \times 10^{-10}$); antibodies to all the remaining T cell integrins failed to decrease tether formation (**Fig. 5a**). This LFA-1 interaction on T cells was achieved mainly through interaction with ICAM-1, as blocking antibody to ICAM-1 led to a 62% reduction in adhesion and the residual adhesion was blocked with antibody to ICAM-2 (**Fig. 5b**). Furthermore, tethered T cells had accumulated LFA-1 at the contacts (**Fig. 5j**).

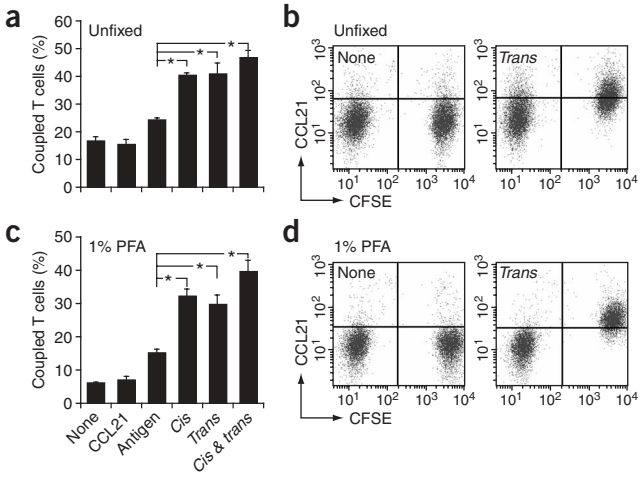

Figure 4 Surface-bound CCL21 presented *in trans* is sufficient to augment antigen-specific coupling of a T cell to a separate APC. DO11.10 T cell blasts were incubated with A20 B cell APCs; 1 μg/ml of OVA peptide and/or CCL21 was prepulsed onto the surface of APCs and cells were washed. Antigen and CCL21 were presented on the same cell (*Cis*) or presented separately on different cells (*Trans*). (**a**) Interaction of T cells with unfixed APCs. (**b**) Flow cytometry for CCL21 expression by unfixed APCs. (**c**) Interaction of T cells with APCs fixed with 1% paraformaldehyde (PFA). (**d**) Flow cytometry for CCL21 expression by APCs fixed with 1% paraformaldehyde. In **a**,**c**, the percentage of T cells interacting with APCs at 15 min was assessed by flow cytometry; *, $P \leq 0.02$ (two-tailed Student's *t*-test); error bars, s.d. of triplicate samples. In **b**,**d**, cell populations were distinguished by labeling with CFSE (5-(and-6)-carboxyfluorescein succinimidyl ester). Data in each panel are representative of three experiments.

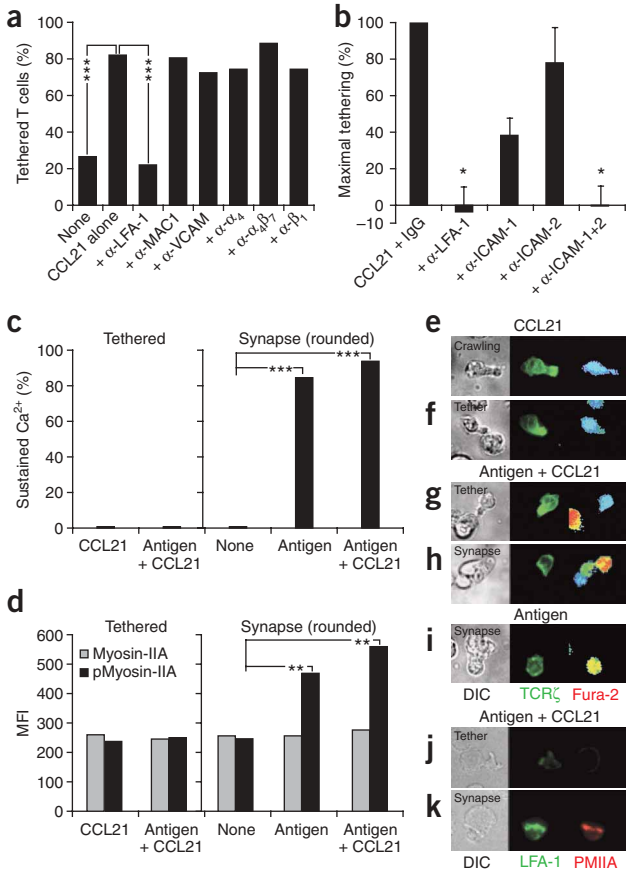

Figure 5 Chemokine-induced tethers are dependent on LFA-1 and ICAM but do not permit TCR-mediated signaling. (**a**) Antibody blockade of CCL21-induced tethering of DO11.10 T cell blasts and A20 APCs preincubated with 10 μg/ml of antibody (horizontal axis; α-, antibody to). ***, $P \leq 1 \times 10^{-9}$, versus CCL21 alone (χ^2 test); $n > 15$ cells per condition. (**b**) Interaction of DO11.10 T cell blasts and A20 B cell APCs preincubated with 20 μg/ml of antibody (horizontal axis), assessed by flow cytometry at 1 min in the presence or absence of 1 μg/ml of CCL21. For normalization between experiments, values for tethering in the absence of added chemokine are subtracted as background. *, $P \leq 0.05$, versus chemokine plus rat IgG (two-tailed Student's *t*-test). Error bars, s.d. of four experiments. (**c**,**d**) Calcium and phospho-myosin IIA content of synapses and tethers. (**c**) Calcium flux of DO11.10 T cell blasts incubated in the presence (Antigen) or absence (None) of 1 μg/ml of OVA peptide and/or 1 μg/ml of CCL21, based on the ratio of Fura-2AM emission at 340 nm versus at 380 nm; flux is considered sustained if it is maintained for 2 min or more. (**d**) Phosphorylation of myosin-IIA (pMyosin-IIA) in DO11.10 T cell blasts incubated with A20 B cell APCs in the presence or absence of 1 μg/ml of OVA peptide and/or 1 μg/ml of CCL21 for 12–15 min, then fixed and stained. **, $P \leq 1 \times 10^{-7}$, and ***, $P \leq 1 \times 10^{-9}$, versus coupled T cells in the absence of OVA peptide or chemokine (χ^2 test; **c**) or versus coupled T cells in the absence of OVA peptide or chemokine (two-tailed Student's *t*-test; **d**). Data are representative of three experiments ($n \geq 25$ (**c**) or $n \geq 22$ (**d**) cells per condition). (**e**–**i**) TCRζ localization and calcium flux intensities of DO11.10 T cell blasts transduced with a green fluorescent protein–TCRζ construct and labeled with Fura-2AM in the presence or absence of 1 μg/ml of OVA peptide and/or 1 μg/ml of CCL21. (**j**,**k**) Staining intensity of LFA-1 and phosphorylated myosin-IIA (PMIIA) and localization in a tether and couple, as described for **d**. Original magnification, ×40. Data are representative of one (**a**), four (**b**) or three (**c**–**j**) experiments.

Chemokine engagement inhibits TCR signaling

Based on our microscopy, we defined tethers as consisting of elongated cells anchored by their trailing constricted uropods, but another feature (**Fig. 3a**) was the absence of calcium signaling while in the tethered state. All CCL21-mediated tethers, even on cells copresenting cognate antigen, were unable to support sustained calcium fluxes (**Fig. 5c**). However, cells with synapse morphology derived through one-step (antigen-only) or two-step (antigen-and-CCL21) encounters mediated robust calcium signaling. As another measure of TCR-mediated signaling and stopping, we assessed phosphorylation on Thr1939 of the myosin IIA heavy chain. This event has been shown to 'debundle' complexes of this motor[24] with filamentous actin and is associated with TCR signaling–induced disassembly of the uropod in T cells[13]. T cells in chemokine-mediated tethers had small amounts of myosin-IIA phosphorylated at Thr1939 (**Fig. 5d**,**j**). In contrast, cells that had converted to a synapse morphology, either after tethering or directly in the absence of chemokines, had more myosin-IIA phosphorylated at Thr1939 (**Fig. 5d**,**k**).

Finally, we assessed synapse TCR-CD3ζ localization in T cells that were tethered and had formed synapses. T cells in tethers maintained a uropod-localized pool of green fluorescent protein–labeled TCR-CD3ζ (**Fig. 5f**,**g**), as did crawling cells (**Fig. 5e**), thus negating the argument that the TCR was somehow polarized away from the contact site. However, T cells with synapse morphology (**Fig. 5h**) had central supramolecular activating clusters of TCR-CD3ζ similar to those that formed in the absence of chemokines (**Fig. 5i**). Thus, chemokine-mediated tethers are consistent with the idea of a 'holding pattern' in which the cell has not yet initiated TCR signaling.

Naive T cells are captured by chemokine-bearing APCs

Our model system was useful for elucidating how chemokines function in T cell–APC interactions to augment T cell antigen reactivity; however, it was also important to show that this mechanism was relevant to naive T cells. Thus, we examined naive T cell tethering in response to CCL21 using real-time microscopy as in **Figure 2a**,**b**. We noted similar frequencies of CCL21-induced tethering in naive DO11.10 T cells (42%) (**Fig. 6a**) and T cells blasts (**Fig. 2b**), given that naive cells had very low frequencies of background tethering (4%) (**Fig. 6a**) in the absence of added chemokine. During tethering, naive T cells became intermittently polarized and rounded but remained attached to the APC. That morphology was reminiscent of that of

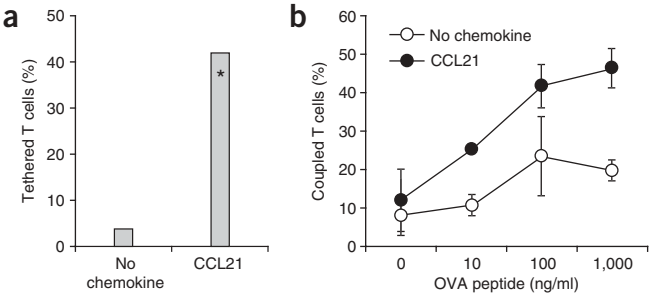

Figure 6 Naive T cells are captured by APCs in the presence of CCL21, resulting in improved antigen-specific coupling. (**a**) Quantification of tethering of naive DO11.10 T cells to A20 B cell APCs in the presence or absence of 1 μg/ml of CCL21 (representative video, **Supplementary Video 5**). *, $P < 1 \times 10^{-9}$, versus samples with no chemokine (χ^2 test). Data are pooled from two experiments ($n > 80$ cells per condition). (**b**) Coupling of naive DO11.10 T cells and A20 B cell APCs incubated together with OVA peptide (concentration, horizontal axis) in the presence (CCL21) or absence (No chemokine) of 1 μg/ml of CCL21, assessed by flow cytometry at 15 min. Error bars, s.d. of two experiments. Data are representative of two (**a**) or four (**b**) experiments.

crawling naive T cells as seen by two-photon microscopy, in which bursts of crawling were interrupted by stationary periods with rounded morphology[1,25] (**Supplementary Video 5** online).

To determine if the CCL21-induced augmentation of coupling in T cell blasts occurred in naive T cells, we used the flow cytometry–based cell-coupling assay. We incubated naive DO11.10 T cells with A20 B cell APCs in the presence of cognate antigen or CCL21 or both and after 15 min assessed the proportion of T cell–APC couples formed using a range of peptide concentrations. The presence of CCL21 augmented coupling efficiencies in naive T cells approximately twofold over a range of peptide concentrations (**Fig. 6b**).

Consistent with published reports[17], CCL21 also augmented the proliferation of naive DO11.10 T cells in response to splenocyte APCs, resulting in an augmentation in proliferation of two- to threefold over that in absence of the chemokine (**Supplementary Fig. 1** online). That proliferative augmentation was due to a chemokine effect on T cells, as it was fully blocked by pretreatment of the T cells with pertussis toxin (**Supplementary Fig. 1**). In conclusion, our results have suggested that a local effect of bound chemokine in distinct zones of lymph nodes may mediate increased dwell times and reactivity there (**Supplementary Fig. 2** online).

DISCUSSION

In this report, we have described a two-step dynamic for T cell–APC interactions in the presence of chemokines. Our results were unexpected, as they showed that chemokines were directly 'presented' by putative APCs or neighboring cells and that this form of chemokine influenced T cell motility and subsequent T cell reactivity. We have demonstrated here the dynamics of chemokine costimulation by microscopy. In particular, we have shown both the establishment of a transient tether with highly polarized morphology and the very rapid and efficient release of that tether after subsequent antigen engagement.

We believe that the function of the chemokine-induced two-step T cell activation is to promote T cell activation in a 'neighborhood' of appropriately chemokine-tagged APCs through two mechanisms. First, the tether captures the T cell for a period of time, resulting in more extensive localized 'scanning'. Second, the resulting polarized T cell has a higher probability of stable antigen-dependent interactions with nearby APCs because of increased sensitivity to antigen.

What happens in the T cell during this adherent tethered contact? Like an immunological synapse, the chemokine-induced tether required LFA-1 and had TCR localized toward the contact. However, it differed substantially from the antigen-mediated contact, because the T cell maintained an elongated amoeboid form and did not promote appreciable calcium release or myosin motor phosphorylation, and the contact maintained the TCR diffusely around the uropod and not in a classical aggregation of central supramolecular activating clusters. Although CCR7 signaling promotes some calcium signal in transfectants, the reported magnitude of calcium release is an order of magnitude weaker than that induced by the TCR[26]. Those data suggest that the tethered T cell is essentially a T cell that is continuing to try to crawl away but is bound by its uropod. Polarized amoeboid T cells have been shown to have a 'preference' for stimulation at their leading edge[12,27]. We suggest that the tether is a hyperpolarized T cell with resulting enhanced sensitivity to antigen at the leading edge.

Another key finding here was the cell surface display of chemokines in the lymph node, 'preferentially' on DCs. Chemokines are highly charged molecules that bind to heparin (which binds to the extracellular matrix) and proteins modified with glycosaminoglycans[28]. The lymphoid chemokines CCL19 and CCL21 are made by the stroma, high endothelial venules and DCs[4], and glycosaminoglycans are probably present on those surfaces[20]. We have shown that DCs bound more CCL21 on their surface than did B cells and T cells, suggesting that DCs either have higher expression of glycosaminoglycans or have increased access to the chemokine because of their localization *in vivo*. Modulation of the glycosaminoglycan content on those surfaces may provide a mechanism for increasing T cell sampling and for priming T cells for activation in that local 'neighborhood'. Tethering on APCs seems to represent an activity analogous to arrest of lymphocytes on high endothelial venules in an alternative environment and for a different purpose.

As chemokine-dependent augmentation of antigen reactivity was as effective *in trans* as it was *in cis*, we suggest that tethering on chemokine-bearing surfaces such as DCs, stromal cells[29] or high endothelial venules in the T cell zone could serve to increase surveillance of and sensitivity to local DCs. Longer dwell times and enhanced reactivity induced by tethering would result in increased scanning of and sensitivity to all APCs in the chemokine-rich 'neighborhood'. An attractive feature of this model is that the CCR7 ligands that induce tethering also attract mature DCs[29,30], thereby capturing T cells in an area rich with activated antigen-loaded DCs. Regulation of CCR7 expression has been noted after TCR stimulation[31,32], and such modulation may promote the ability of stimulated cells to interact in those locales.

The 'choreography' of a two-step mechanism of T cell activation that leads to increased antigen responsiveness expands the known function of these chemokines. Studies have suggested that the 'dominant' chemokines CCL19, CCL21 and CXCL10 block the 'arrest' of T cells on peptide-MHC complexes[19] and that a supported lipid bilayer bearing ICAM, peptide-MHC and immobilized CCL21 augments antigen-dependent adhesion[23]. Another report has shown that 'subordinate' chemokines binding CCR5 and CXCR4 can costimulate T cell function and have suggested this occurs through polarization of chemokine signaling into the synapse[18]. However, that mechanism does not account for the demonstrated costimulation of dominant CCL21 (ref. 17), whose chemokine receptor is not present in the synapse[18]. Our data have addressed the apparent conundrum concerning the function of CCL21 and other 'dominant' chemokines in promoting T cell activation. Additional work has shown that CCL19 increases the rate of T cell motility on high-density monolayers of DCs and has suggested that this allows T cells to scan more total APCs and thus find rare antigens[33]. Our data have not excluded the possibility of chemokine-induced motility as mechanism for increased scanning of APCs. Instead, our results have provided evidence of an additional mechanism for increasing local scanning through T cell capture and have demonstrated that chemokines augment antigen recognition in seemingly optimal conditions with an abundance rather than scarcity of antigen-bearing APCs.

Finally, our work 'predicts' that the previously characterized 'random walk' of T cells in the lymph node will prove to have chemokine-modulated organization. That has become apparent for CCR7-mediated recruitment of B cells to the T cell zone[34] and also for CCL3- and CCL4-mediated recruitment of CD8 T cells to $CD4^+$ T cell–bound DCs[35]. Our demonstration of cell surface capture has also suggested that the periodic motility and pausing of T cells *in vivo*[1,25] is probably directed not simply by a gradient (front to back) of soluble chemokines but also by individual adhesive interactions between the leading edge and/or uropod.

Confirmation of those ideas will require continued and detailed analysis of T cell motility relative to specific features of the lymph node. Other published random walk motility measurements have not included visualization of DCs or other chemokine-bearing surfaces.

Our data predict that in some cases, rather than including only chemokine-mediated directional motility, there will also be consistent pause points in the regions where these chemokines and integrin ligands are optimally presented, leading to a corresponding likelihood of activation there.

METHODS

Mice and cells. BALB/c mice, C57BL/6 mice and transgenic mice expressing the DO11.10 TCR specific for chicken ovalbumin amino acids 323–339 (called 'OVA peptide' here) in the context of the MHC class II molecule I-A^d were purchased from The Jackson Laboratory. DO11.10 mice were crossed with BALB/c mice to obtain heterozygous DO11.10 mice. CCR7-deficient mice[30] were obtained from M. Lipp (Max-Delbruck-Center for Molecular Medicine, Berlin, Germany). All mice were bred and maintained in accordance with the guidelines of the Lab Animal Resource Center of the University of California at San Francisco (San Francisco, California). The A20 B cell APC line has been described[13]. DO11.10 T cell blasts were obtained by stimulation of cells from DO11.10 spleen and peripheral lymph nodes with 1 μg/ml of OVA peptide and culture of cells with 1–2 U/ml of interleukin 2 after day 2 of stimulation. C57BL/6 or CCR7-deficient blasts were obtained by stimulation of spleen and lymph node cells with 1 μg/ml of staphylococcal enterotoxin B and culture of cells with 1–2 U/ml of interleukin 2 after day 2 of stimulation. Naive $CD4^+$ DO11.10 T cells were isolated with the CD4 negative selection kit (Miltenyi).

Antibodies and chemokines. Anti-LFA-1 (M17/4), allophycocyanin-conjugated anti-CD4 (GK1.5), fluorescein isothiocyanate–conjugated anti-CD40 (FGK45.6), anti-Mac-1 (M1/70), anti–vascular cell adhesion molecule (M29 and M/K-2), anti–integrin α_4 (R1-2 and 9C10), anti–integrin $\alpha_4\beta_7$ (DATK32), anti–integrin β_1 (HMB1-1), anti-ICAM-1 (3E2), anti-ICAM-2 (3C4) and control anti-CD8 rat IgG (53.6.72) were obtained from BD Pharmingen. Antibodies for myosin staining included anti-myosin-IIA (Biogenesis 6490-4646) and antibody to myosin-IIA phosphorylated at Thr1939 (ref. 13). Fluorescein isothiocyanate–conjugated donkey anti-rat (712-096-153), rhodamine-conjugated donkey anti-rabbit (711-166-152), fluorescein isothiocyanate–conjugated donkey anti-goat (705-096-147), allophycocyanin-conjugated donkey anti-goat (705-136-147) and goat IgG (005-000-003) were all from Jackson ImmunoResearch. All experiments used synthetic chemokines; CCL21 and CCL19 were obtained from Peprotech; and CCL3, CXCL10, CCL5, CCL17 and CXCL12 and anti-CCL21 (AF457) were obtained from R&D Systems.

Microscopy. A modified Zeiss Axiovert 200M microscope with a plan-neofluar 40× objective (Carl Zeiss) was used for imaging experiments. The microscope was fitted with dual excitation and emission filter wheels and a Photometrics Coolsnap-HQ camera. The imaging and control software used was Metamorph (Universal Imaging). For imaging of live morphology, T cell blasts or naive DO11.10 T cells were 'loaded' for 10 min at 37 °C with 1 μM Fura-2, AM (Molecular Probes) and were washed. T cells (2×10^5 to 4×10^5) and A20 B cell APCs (1×10^5) were plated in coverslip wells (Nunc) in RPMI medium (Gibco) containing 10% FBS (HyClone) and 0.25% low-melting-point agarose (BMA). OVA peptide (1 μg/ml) and/or CCL21 or CCL19 (1 μg/ml) were (was) added to cultures where indicated. Cells were incubated for 5 min at 37 °C before imaging and were maintained at 37 °C on the heated stage of the microscope. Data from DIC images, Fura emissions at 340 nm and 380 nm and green fluorescence (for retrovirally transduced cells) were collected at 15- to 30-second intervals over a 10- to 30-minute period. For assays requiring surface-bound chemokine, cells were preincubated for 10 min with CCL21 and were washed two times before T cells and APCs were combined. For antibody-blockade experiments, T cells and APCs were preincubated separately for 10 min with 10 μg/ml of antibody. 'Tethered' cells were identified as having a polarized amoeboid morphology with a constricted uropodal attachment to an APC. Cells with synapses were identified as having a rounded morphology with a flat surface attached to an APC, and, in **Figure 3b**, also as having a sustained calcium influx. Calcium flux was assessed based on the ratio of Fura-2AM emissions at 340 nm to those at 380 nm, with increased ratios indicating calcium flux.

Flow cytometry–based coupling. For assays with OVA peptide and chemokine in the culture, 2×10^5 A20 B cell APCs were preincubated for 10 min at 37 °C with twice the indicated concentration of the OVA peptide and/or chemokine. Subsequently, DO11.10 T cell blasts or naive DO11.10 $CD4^+$ T cells (2×10^5) were added to the APCs in an equal volume. Cells were immediately centrifuged for 1 min at 228*g* and were incubated at 37 °C. After incubation, cells were immediately fixed for 10 min at 37 °C with an equal volume of warm 4% paraformaldehyde (Electron Microscopy Sciences) in PBS and were washed. B cell APCs were stained with fluorescein isothiocyanate–conjugated anti-CD40 and T cells were stained with allophycocyanin-conjugated anti-CD4. Cells were analyzed on a FACSCalibur (Beckton Dickinson) for quantification of the percentage of couple formation, calculated as the number of T cells in the double-positive quadrant ($CD4^+CD40^+$) versus the total number of T cells ($CD4^+$). For assays requiring surface-bound antigen and chemokine, APCs were preincubated for 1 h with chemokine and OVA peptide, were washed two times, were fixed for 5 min at 25 °C in 1% paraformaldehyde in PBS and were washed two additional times before incubation of T cells and APCs together. For assays containing blocking antibodies, T cells and APCs were preincubated separately for 10 min with 20 μg/ml of antibody before T cells and APCs were combined.

Retroviral infection. The CD3ζ–green fluorescent protein retroviral construct[36] was transfected into the Phoenix E packaging cell line (from G. Nolan, Stanford University, Stanford, California). Media were changed on the day after transfection and supernatants were collected on days 2 and 3 after transfection and were used directly for infection. Before infection, 2×10^6 cells obtained from DO11.10 spleen and lymph nodes were cultured for 2 d with 1 μg/ml of OVA peptide in a volume of 1 ml per well of 24-well plates. On days 2 and 3, 1 ml of viral supernatant plus 1 μg/ml of polybrene (Sigma) were added per well. Plates were centrifuged for 30 min at 1,100*g* at 25 °C. On day 5, green fluorescent protein–positive T cells were sorted on a MoFlo high-speed cell sorter (Cytomation).

Immunocytochemistry. Fixed cell staining was done by incubation for 15 min at 37 °C of 2×10^5 DO11.10 T cell blasts together with 1×10^5 A20 B cells APCs on Superfrost slides (VWR). Cells were then fixed for 10 min at 37 °C with 1% paraformaldehyde and were centrifuged to adhere the cells to the slide. Fixed cells were blocked with 3% donkey serum and were made permeable for 30 min with 0.02% saponin (Sigma) in PBS. Cells were incubated for 60 min with primary antibodies, then were washed extensively, followed by secondary antibody staining for 60 min. After thorough washing, cells were treated with antifade reagent (BioRad) and slides were sealed and imaged. Mean fluorescent intensity was measured from the medial *z*-plane with a tight gate drawn around the cell of interest.

Proliferation. Naive DO11.10 CD4 T cells (1×10^4) were cultured with γ-irradiated DO11.10 splenocytes (1×10^5) in 96-well plates. After 48 h, cultures were pulsed for 12–18 h with 1 μCi/well of [^{3}H]thymidine (New England Nuclear) and incorporated radioactivity was measured in a Betaplate scintillation counter (Wallac). OVA peptide and CCL21 were added just before the addition of T cells.

Note: Supplementary information is available on the Nature Immunology website.

ACKNOWLEDGMENTS

We thank J. Cyster, E. Brown and T. Okada for insight and help with reagents; C. Bennett for technical support; S.W. Jiang for flow cytometry; and J. Cyster, S. Rosen and R. Locksley for critical reading of the manuscript.

AUTHOR CONTRIBUTIONS

R.S.F. performed all experiments and data analysis and participated in experimental design and manuscript writing. J.J. assisted with experimental design, some experiments and manuscript writing, provided intellectual guidance and performed blinded quantifications. M.F.K. established the initial scientific questions, provided continuing intellectual guidance and participated in experimental design and manuscript writing.

COMPETING INTERESTS STATEMENT

The authors declare that they have no competing financial interests.

Published online at http://www.nature.com/natureimmunology/
Reprints and permissions information is available online at http://npg.nature.com/reprintsandpermissions/

1. Miller, M.J., Wei, S.H., Parker, I. & Cahalan, M.D. Two-photon imaging of lymphocyte motility and antigen response in intact lymph node. *Science* **296**, 1869–1873 (2002).
2. Mempel, T.R., Henrickson, S.E. & von Andrian, U.H. T-cell priming by dendritic cells in lymph nodes occurs in three distinct phases. *Nature* **427**, 154–159 (2004).
3. Miller, M.J., Safrina, O., Parker, I. & Cahalan, M.D. Imaging the single cell dynamics of CD4$^+$ T cell activation by dendritic cells in lymph nodes. *J. Exp. Med.* **200**, 847–856 (2004).
4. Cyster, J.G. Chemokines and cell migration in secondary lymphoid organs. *Science* **286**, 2098–2102 (1999).
5. Wülfing, C. *et al.* Kinetics and extent of T cell activation as measured with the calcium signal. *J. Exp. Med.* **185**, 1815–1825 (1997).
6. Lee, K.H. *et al.* T cell receptor signaling precedes immunological synapse formation. *Science* **295**, 1539–1542 (2002).
7. Grakoui, A. *et al.* The immunological synapse: A molecular machine that controls T cell activation. *Science* **285**, 221–226 (1999).
8. Krummel, M.F., Sjaastad, M.D., Wülfing, C. & Davis, M.M. Differential assembly of CD3ζ and CD4 during T cell activation. *Science* **289**, 1349–1352 (2000).
9. Wulfing, C. *et al.* Costimulation and endogenous MHC ligands contribute to T cell recognition. *Nat. Immunol.* **3**, 42–47 (2002).
10. Monks, C.R., Freiberg, B.A., Kupfer, H., Sciaky, N. & Kupfer, A. Three-dimensional segregation of supramolecular activation clusters in T cells. *Nature* **395**, 82–86 (1998).
11. Dustin, M.L., Bromley, S.K., Kan, Z., Peterson, D.A. & Unanue, E.R. Antigen receptor engagement delivers a stop signal to migrating T lymphocytes. *Proc. Natl. Acad. Sci. USA* **94**, 3909–3913 (1997).
12. Negulescu, P.A., Krasieva, T.B., Khan, A., Kerschbaum, H.H. & Cahalan, M.D. Polarity of T cell shape, motility, and sensitivity to antigen. *Immunity* **4**, 421–430 (1996).
13. Jacobelli, J., Chmura, S.A., Buxton, D.B., Davis, M.M. & Krummel, M.F. A single class II myosin modulates T cell motility and stopping but not synapse assembly. *Nat. Immunol.* **5**, 531–538 (2004).
14. Laudanna, C., Campbell, J.J. & Butcher, E.C. Role of Rho in chemoattractant-activated leukocyte adhesion through integrins. *Science* **271**, 981–983 (1996).
15. Campbell, J.J. *et al.* Chemokines and the arrest of lymphocytes rolling under flow conditions. *Science* **279**, 381–384 (1998).
16. Constantin, G. *et al.* Chemokines trigger immediate β_2 integrin affinity and mobility changes: differential regulation and roles in lymphocyte arrest under flow. *Immunity* **13**, 759–769 (2000).
17. Flanagan, K., Moroziewicz, D., Kwak, H., Horig, H. & Kaufman, H.L. The lymphoid chemokine CCL21 costimulates naive T cell expansion and Th1 polarization of non-regulatory CD4$^+$ T cells. *Cell. Immunol.* **231**, 75–84 (2004).
18. Molon, B. *et al.* T cell costimulation by chemokine receptors. *Nat. Immunol.* **6**, 465–471 (2005).
19. Bromley, S.K., Peterson, D.A., Gunn, M.D. & Dustin, M.L. Cutting edge: hierarchy of chemokine receptor and TCR signals regulating T cell migration and proliferation. *J. Immunol.* **165**, 15–19 (2000).
20. Rot, A. Neutrophil attractant/activation protein-1 (interleukin-8) induces *in vitro* neutrophil migration by haptotactic mechanism. *Eur. J. Immunol.* **23**, 303–306 (1993).
21. Proudfoot, A.E. *et al.* Glycosaminoglycan binding and oligomerization are essential for the *in vivo* activity of certain chemokines. *Proc. Natl. Acad. Sci. USA* **100**, 1885–1890 (2003).
22. Shamri, R. *et al.* Lymphocyte arrest requires instantaneous induction of an extended LFA-1 conformation mediated by endothelium-bound chemokines. *Nat. Immunol.* **6**, 497–506 (2005).
23. Bromley, S.K. & Dustin, M.L. Stimulation of naive T-cell adhesion and immunological synapse formation by chemokine-dependent and -independent mechanisms. *Immunology* **106**, 289–298 (2002).
24. Dulyaninova, N.G., Malashkevich, V.N., Almo, S.C. & Bresnick, A.R. Regulation of myosin-IIA assembly and Mts1 binding by heavy chain phosphorylation. *Biochemistry* **44**, 6867–6876 (2005).
25. Friedman, R.S., Jacobelli, J. & Krummel, M.F. Mechanisms of T cell motility and arrest: deciphering the relationship between intra- and extracellular determinants. *Semin. Immunol.* **17**, 387–399 (2005).
26. Ngo, V.N., Tang, H.L. & Cyster, J.G. Epstein-Barr virus-induced molecule 1 ligand chemokine is expressed by dendritic cells in lymphoid tissues and strongly attracts naive T cells and activated B cells. *J. Exp. Med.* **188**, 181–191 (1998).
27. Wei, X., Tromberg, B.J. & Cahalan, M.D. Mapping the sensitivity of T cells with an optical trap: Polarity and minimal number of receptors for Ca^{2+} signaling. *Proc. Natl. Acad. Sci. USA* **96**, 8471–8476 (1999).
28. Lau, E.K. *et al.* Identification of the glycosaminoglycan binding site of the CC chemokine, MCP-1: implications for structure and function *in vivo*. *J. Biol. Chem.* **279**, 22294–22305 (2004).
29. Luther, S.A., Tang, H.L., Hyman, P.L., Farr, A.G. & Cyster, J.G. Coexpression of the chemokines ELC and SLC by T zone stromal cells and deletion of the ELC gene in the *plt/plt* mouse. *Proc. Natl. Acad. Sci. USA* **97**, 12694–12699 (2000).
30. Forster, R. *et al.* CCR7 coordinates the primary immune response by establishing functional microenvironments in secondary lymphoid organs. *Cell* **99**, 23–33 (1999).
31. Sallusto, F. *et al.* Switch in chemokine receptor expression upon TCR stimulation reveals novel homing potential for recently activated T cells. *Eur. J. Immunol.* **29**, 2037–2045 (1999).
32. Langenkamp, A. *et al.* Kinetics and expression patterns of chemokine receptors in human CD4$^+$ T lymphocytes primed by myeloid or plasmacytoid dendritic cells. *Eur. J. Immunol.* **33**, 474–482 (2003).
33. Kaiser, A., Donnadieu, E., Abastado, J.P., Trautmann, A. & Nardin, A. CC chemokine ligand 19 secreted by mature dendritic cells increases naive T cell scanning behavior and their response to rare cognate antigen. *J. Immunol.* **175**, 2349–2356 (2005).
34. Okada, T. *et al.* Antigen-engaged B cells undergo chemotaxis toward the T zone and form motile conjugates with helper T cells. *PLoS Biol.* **3**, e150 (2005).
35. Castellino, F. *et al.* Chemokines enhance immunity by guiding naive CD8$^+$ T cells to sites of CD4$^+$ T cell-dendritic cell interaction. *Nature* **440**, 890–895 (2006).
36. Richie, L.I. *et al.* Imaging synapse formation during thymocyte selection: inability of CD3ζ to form a stable central accumulation during negative selection. *Immunity* **16**, 595–606 (2002).

Corrigendum: Surface-bound chemokines capture and prime T cells for synapse formation

Rachel S Friedman, Jordan Jacobelli & Matthew F Krummel

Nature Immunology **7**, 1101–1108 (2006); published online 10 September 2006; corrected after print 29 September 2006

In the version of this article initially published, the label at the far right of the horizontal axis of **Figure 5a** is incorrect. The correct label should be α-β_1. The error has been corrected in the PDF version of the article.

Corrigendum: Clonal deletion of thymocytes by circulating dendritic cells homing to the thymus

Roberto Bonasio, M Lucila Scimone, Patrick Schaerli, Nir Grabie, Andrew H Lichtman & Ulrich H von Andrian

Nature Immunology **7**, 1092–1100 (2006); published online 3 September 2006; corrected after print 29 September 2006

In the version of this article initially published, the third sentence in the legend of Figure 6 is incorrect. The correct sentence should read "*, $P < 0.01$, and **, $P < 0.001$, compared with DCs". In the last sentence of the legend to Figure 8, 'obtainted' should read 'obtained'. On page 1098, in the first sentence of the first full paragraph, 'fused' should read 'used'. These errors have been corrected in the HTML and PDF versions of the article.